Journal of Petroleum Science and Engineering 126 (2015) 124–130

Contents lists available at ScienceDirect

Journal of Petroleum Science and Engineering

journal homepage: www.elsevier.com/locate/petrol

Determining the elastic constants of hydrocarbons of heavy oil products using molecular dynamics simulation approach

Maksym S. Stetsenko*

Marine Engineering Faculty, Odesa National Maritime Academy, 13, Didrikhson Street, Odesa 65029, Ukraine

ARTICLE INFO

Article history:
Received 26 July 2013
Accepted 23 December 2014
Available online 2 January 2015

Keywords:
n-Paraffin
Molecular Dynamics
Elastic Constants

ABSTRACT

We have performed a molecular dynamics study in order to verify the assumption that saturated hydrocarbons can be characterized by generalized Hook's law using the fourth rank tensor of elastic constants. In this study normal paraffins were treated as crystals of hexagonal symmetry. Thus, we obtained original numerical values of Young's modulus and Poisson's ratio in both anisotropic and isotropic planes and the values of the shear modulus at three different temperatures.

Negative Poisson's ratio of n-paraffins is of a particular interest. The author believes that auxetic behavior of saturated hydrocarbons is the result of their liquid-crystalline nature. Another remarkable point is the non-linear elasticity of n-paraffins detected in a wide temperature range. This provides an additional experimental confirmation of the phase transition process of hydrocarbons earlier reported in scientific works.

We have shown that the matrix of elasticity of a particular heavy petroleum product can be estimated using the elastic parameters of the n-paraffins obtained. The numerical values of five independent elastic constants are directly proportional to the composition of a heavy petroleum product. The simplified representation of the composition can be defined by a few saturated hydrocarbons with different carbon numbers.

The numerical results obtained in this research may be useful for those interested in heavy petroleum fractions rheology as well as those who perform numerical studies in petroleum hydrodynamics and acoustics.

1. Introduction

The analysis performed in publications dedicated to oil and oil products structural properties resulted in establishing the fact that highly viscous oil products (such as heavy fuel oil) belong to periodic dispersion mediums (Leffler, 1985; Venkatesan et al., 2005; Bagheri et al., 2010; Speight, 2014). The solid phase in those is formed by the normal and dehydrated paraffin molecules with a high number of carbon atoms.

However, in most of the hydrodynamical and fluid–structure interaction calculations and studies heavy oil products are still considered homogeneous or viscoelastic liquids. That is due to the lack of fundamental research of the elastic properties of heavy oil products crystalline structures.

One way to determine the elastic properties of a material is to use the technical means of research. Ultrasonic waves propagation measuring units, X-ray laboratory systems and atomic force microscopes are used for this purpose. At the same time such equipment requires significant financial costs and can be unavailable for a big group of researchers.

Another way is to use the computational means for research. A method of modeling the interatomic forces in organic crystals is described below. The author has proposed an approach to determining the elastic constants of some normal paraffin (n-paraffin) crystals. Those constants, in a first approximation, can be used for estimating heavy oil products elasticity.

Elastic constants characterize the stiffness of a material. The formal definition is provided by a linear relation that holds between the stress and strain tensors in the limit of an infinitesimal deformation. In tensor notation, this is expressed as where the repeated indices imply summation. s_{ij} are the elements of the symmetric stress tensor, e_{kl} are the elements of the symmetric strain tensor. C_{ijkl} are the elements of the fourth rank tensor of elastic constants. In three dimensions, this tensor has $3^4=81$ elements. Using Voigt notation, the tensor can be written as a 6×6 matrix, where c_{ij} is now the derivative of s_i with respect to e_i. Because s_i is itself a derivative w.r.t. e_i, it follows that c_{ij} is also symmetric, with at most=21 distinct elements. The number of

---

* Tel.: +380 637714848.
E-mail addresses: directm.od@rambler.ru, ms.stetsenko@gmail.com

http://dx.doi.org/10.1016/j.petrol.2014.12.021

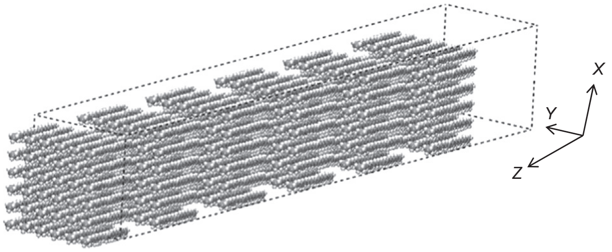

Fig. 1. Crystal structure of $C_{24}H_{50}$.

elastic constants is further reduced if the crystal structure of the material has a certain type of symmetry (Ding et al., 2006).

2. Structures and methods

2.1. Structural properties of n-paraffins

There are three low-temperature crystalline modifications of n-paraffins: orthorhombic, monoclinic and triclinic. Their diversity is defined by the number of carbon atoms (length of the molecule) and the parity of the number (the symmetry of molecular chains). The example of an n-paraffin with a triclinic symmetry is illustrated in Fig. 1 which shows a 6 × 6 × 6 three-dimensional model of tetracosane (chemical formula: $C_{24}H_{50}$) as well as its dimensional properties. The dimensions and types of the symmetry of the unit cell of this and other saturated hydrocarbons can be found in Kotelnikova and Filatov (2002).

2.2. Methods

An accurate representation of the potential energy lies at the heart of all the simulations of real materials. The accurate potentials are required for molecular simulations to predict the behavior and properties of materials accurately. Qualitative conclusions drawn from simulations employing inaccurate or unvalidated potentials are problematic.

At zero temperature, it is easy to estimate the derivatives c_{ij} by deforming the cell in one of the six directions and measuring the change in the stress tensor as this option is normally available in any molecular dynamics simulation code.

Calculating elastic constants at a finite temperature is more challenging because it is necessary to run a simulation that performs time averages of differential properties. One way to do this is to measure the change in average stress tensor in a normal volume and temperature (NVT) simulation when the cell volume undergoes a finite deformation. In order to balance the systematic and statistical errors in this method, the magnitude of the deformation must be chosen judiciously, and care must be taken to fully equilibrate the deformed cell before sampling the stress tensor. Another approach is to sample the triclinic cell fluctuations that occur in a normal pressure and temperature (NPT) simulation. This method can also be slow to converge and requires careful post-processing (Yip, 2005).

3. Force field theory

3.1. Force fields for organic molecules simulation

In general, force fields can be divided into three categories: (a) parameterized force fields based upon a broad training set of molecules such as small organic molecules, peptides, or amino acids including AMBER (Cornell et al., 1995), COMPASS (Sun, 1998), OPLS-AA (Jorgensen et al., 1996) and CHARMM (MacKerell et al., 1998); (b) generic potentials such as DREIDING (Mayo et al., 1990) and UNIVERSAL (Rapp´e et al., 1992) that are not parameterized to reproduce properties of any particular set of molecules; and (c) specialized force fields carefully parameterized to reproduce properties of a specific compound. During the past 10 years, the number of research works in organic molecules structure and behavior has significantly increased. In order to provide good quality organic molecule simulations, several force fields have been developed.

For more information about various forms of classical potentials (force fields) for polymers and organic materials, readers can consult Yip (2005).

As the DREIDING force field is characterized as useful for predicting organic crystal structures and dynamics (see for example, Mayo et al., 1990; Diallo et al., 2000), it was used in all the simulation of the research.

3.2. Energy representation in the DREIDING force field

The potential energy for an arbitrary geometry of a molecule is expressed as a superposition of valence (or bonded) interactions (E_{val}) that depend on the specific connections (bonds) of the structure and nonbonded interactions (E_{nb}) that depend only on the distance between the atoms (Mayo et al., 1990; Yip, 2005)

$$E = E_{val} + E_{nb}. \tag{1}$$

In DREIDING the valence interactions consist of bond stretch (E_B, two-body), bond-angle bend (E_A, three-body), dihedral angle torsion (E_T, four-body), and inversion terms (E_I, four-body)

$$E_{val} = E_B + E_A + E_T + E_I, \tag{2}$$

while the nonbonded interactions consist of van der Waals or dispersion (E_{vdw}), electrostatic (E_Q) and explicit hydrogen bonds (E_{hb}) terms

$$E_{nb} = E_{vdw} + E_Q + E_{hb}. \tag{3}$$

The total bond energy is a sum over all bonds. Number of bonds is typically very close to the number of atoms. DREIDING describes the bond stretch interaction either as a simple harmonic oscillator (Mayo et al., 1990)

$$E_B = \sum_{N_{bonds}} \frac{1}{2} k_e (R - R_e)^2 \tag{4}$$

or as the Morse function

$$E_B = \sum_{N_{bonds}} D_e \left[e^{-(\alpha n R - R_e)} - 1 \right]^2. \tag{5}$$

For two bonds *IJ* and *JK* sharing a common atom the three-body angle bend terms are all taken of the harmonic cosine form

$$E_B = \sum_{Nangles} \frac{1}{2} C_{IJK} \left(\cos\, \theta_{IJK} - \cos\, \theta^0_{IJK} \right)^2, \tag{7}$$

where θ is the angle between bonds *IJ* and *JK*. The equilibrium angles are assumed independent of *I* and *K*.

The torsion interaction for two bonds *IJ* and *KL* connected via a common bond *JK* is taken of the form

$$E_T = \sum_{Ntorsions} \sum_{n=1}^{n_{JK}} \frac{1}{2} V_{JK} \left\{ 1 - \cos \left[n_{JK} \left(\phi - \phi^0_{JK} \right) \right] \right\}, \tag{8}$$

where φ is the dihedral angle (angle between the *IJK* and *JKL* planes), n_{JK} is the periodicity (an integer), V_{JK} is the barrier to rotation (always positive), and $\varphi^0_{JK}$is the equilibrium angle.

In DREIDING the torsional parameters are based on hybridization and are independent of the particular atoms involved (Mayo et al., 1990).

The most complex term in a typical organic force field is the inversion term, which is added to ensure that a particular atom *I*, which is bonded to three other atoms *J*, *K*, *L*, remains planar or non-planar.

It is necessary to include an energy term describing how difficult it is to force all three bonds into the same plane (inversion) or how favorable it is to keep the bonds in the same plane.

Denoting the angle between the *IL* bond and the *JIK* plane as ψ, spectroscopists have often used the form

$$E_I = \sum_{Ninv} \frac{1}{2} K_{inv} (\psi - \psi_0)^2. \tag{9}$$

In order that the energy have zero slope for planar configurations ($\psi \to 180^\circ, 0^\circ$), Eq. (9) is replaced with the form

$$E^d_{IJKL} = \sum_{Ninv} \frac{1}{2} C_I (\cos\psi - \cos\psi_I^0)^2, \tag{10}$$

where

$$C_I = K_I / (\sin\psi_I^0)^2 \tag{11}$$

and K_I is the force constant.

The number of valence interactions that must be calculated for a molecule is usually proportional to the number of atoms *n*. The number of nonbonded terms however is roughly proportional to n^2, because they involve almost all possible pairs of atoms.

Both van der Waals and electrostatic interactions are calculated over pairs of atoms, so they are usually done concurrently (Mayo et al., 1990; Yip, 2005).

$$E_{vdw} + E_Q = \sum_i \sum_{j>i} \left\{ (322.0637) Q_i Q_j / \varepsilon R_{ij} + D_0 \left[\left(\frac{R_0}{R_{ij}} \right)^{12} - 2 \left(\frac{R_0}{R_{ij}} \right)^6 \right] \right\}, \tag{14}$$

where R_0 is the van der Waals bond length (Å), D_0 is the van der Waals well depth (kcal/mol), Q_i and Q_j are the charges in electron units, *R* is the distance in Å, ε is the dielectric constant (usually $\varepsilon = 1$) and 332.0637 converts *E* to kcal/mol.

DREIDING treats hydrogens in a special way (Mayo et al., 1990). Hydrogens are not given charges or van der Waals parameters, so Eq. (14) does not apply at all. This is to eliminate errors possible when using the van der Waals parameters appropriate for non-hydrogen-bonded systems.

As a result, the DREIDING force field has a special hydrogen bond term for D–H–A interactions, where D is the hydrogen bond donor, H is the hydrogen bonded to it covalently, and A is the hydrogen bond acceptor, non-covalently attached as shown in Fig. 2. The DREIDING hydrogen bond uses both a radial R_{DA} and an angular θ_{DHA} part:

$$E_{hb} = \sum_i \sum_{j>i} D_{hb} \left[5 \left(\frac{R_{hb}}{R_{AD}} \right)^{12} - 6 \left(\frac{R_{hb}}{R_{AD}} \right)^{10} \cos^4 \theta_{ADH} \right]. \tag{15}$$

Both the radial and angular parts are set to zero beyond certain cutoff values and switching functions are used to make the transition to $E_{hb} = 0$ smooth.

The values of R_{hb} and D_{hb} depend on the convention for assigning charges.

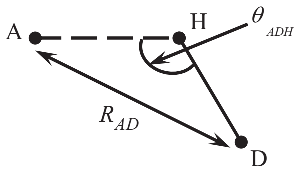

Fig. 2. Hydrogen bonding interpretation.

4. Experimental procedure

4.1. Building experimental models

Molecular dynamics simulations were performed for normal paraffin crystal structures built by a certain number of chains. The size of the chain depends on the number of carbon atoms in a molecule. Long chains can be dozens angstrom in length. The distance between neighbor carbon atoms C–C for n-paraffins is equal to 2.55–2.54 Å (Kotelnikova and Filatov, 2002).

There were three n-paraffins selected for simulation: $C_{19}H_{40}$, $C_{24}H_{50}$ and $C_{36}H_{74}$. The reason is that they are responsible for the composition of heavy petroleum fractions. The structural properties of n-paraffins depend on their composition and H/C ratio. As can be seen from Table 1, the mass of carbon takes approximately 85% in molecules of n-paraffin; H/C ratio remains around 2.1.

The simulation models of hydrocarbons were built with the use of computer software called Materials and Processes Simulation (MAPS). Each model was obtained by the multiplication of the original unit cell which was formed according to the data from Kotelnikova and Filatov (2002). For crystal lattices of n-paraffins $C_{24}H_{50}$ (Fig. 1) and $C_{36}H_{74}$ the number of molecules was 216, and for $C_{19}H_{40}$: 512. These numbers should indicate an evidence of good experimental setup. The total number of atoms in simulation models (Table 2) was two thousand at an average.

n-Paraffins with triclinic, monoclinic and orthorhombic symmetry require simulation in three dimensions: *x*, *y* and *z*; however in this research simulation was conducted in the directions *x* and *z* only. The validity of such simplification was justified by Kotelnikova and Filatov (2002), as authors reported that n-paraffins raise their symmetry up to hexagonal with the increase of temperature.

4.2. Simulation

All the simulations were performed using the classical molecular dynamics code called LAMMPS (Plimpton, 1995) in the form of a plug-in of the MAPS program. It can be used for modeling atomic, polymeric, biological, metallic, granular and coarse-grained systems using a variety of force fields and boundary conditions in a common framework.

In the most general sense, LAMMPS integrates Newton's equations of motion for the collections of atoms, molecules or macroscopic particles that interact via short- or long-range forces with a variety of initial and/or boundary conditions.

Table 1
Composition properties of some hydrocarbons.

Molecule	Mass (g/mole)	% C	% H	H/C
$C_{19}H_{40}$	268.59	85	15	2.1
$C_{24}H_{50}$	338.74	85	15	2.08
$C_{36}H_{74}$	507.1	85.3	14.7	2.06

Table 2
Lattice parameters of some n-paraffins.

n-Paraffin lattice	Mass (g/mole)	Atom number	Volume (Å^3)	*a* (Å)	*b* (Å)	*c* (Å)	α	β	γ
$C_{19}H_{40}$	137,518.1	30,208	468,873.6	312.2	31.6	47.5	90°	90°	90°
$C_{24}H_{50}$	73,167.8	15,984	276,400.5	396	28.7	25.5	91°	96°	106.1°
$C_{36}H_{74}$	109,533.6	23,760	825,940	555.1	33.4	44.5	90°	90°	90°

Newton's equation of motion for an arbitrary atom can be written as

$$m_i \frac{d^2 r_i}{dt^2} = F_i(r_1, ..., r_N) = -\partial E(r_1, ..., r_N)/\partial r_i, \tag{16}$$

meaning that force F_i applied to the ith atom can be found by the differentiation of the potential energy E with respect to the corresponding coordinates of the atom.

The form of Eq. (16) is defined by the type of the operational ensemble, i.e. by the methods of temperature and pressure control used in the simulation.

In order to perform elastic constants determination simulations we used isothermal–isobaric (NPT) ensembles with an extended Nose–Hover temperature and pressure control methods. Martyna et al. (1994) and Shinoda et al. (2004) can be referred to for comprehensive reviews of the equations of motion for this and other methods and ensembles.

The simulation begins with the operational parameters assignment. These include the following: (1) cutoff radius (usually takes 10 Å); (2) initial pressure (usually 0 MPa); (3) final pressure (−101.325 MPa, equals to −1000 Atm); (4) temperature at the beginning, during and at the end of the experiment (all three are normally the same; simulation temperatures were the following: 298.15° K, 333.15 K and 373.15 K); (5) duration of the experiment (60–120 ps); (6) time step (1 fs); (7) interval of writing to a file (usually 10 or 20 fs); and (8) force direction (coordinates X, Y, Z).

The default boundary conditions in LAMMPS are the periodic boundary conditions. The idea of periodic boundary conditions (PBC) is to embed the simulation volume or simulation cell into an infinite, periodic array of replicas or images.

The atoms in the replicas are assumed to behave exactly in the same way as the atoms in the original or primary simulation cell (Field, 2007). Because the primary and image cells are identical, it is irrelevant which one of them is regarded as primary and which are the images. This type of periodic arrangement of atoms is fully specified by a set of repeat vectors, k_i, $i=1, 2, 3$ in 3-dimension. The repeat vectors relate positions of atoms in the periodic replicas. Whenever there is an atom at position $\mathbf{r}$ there are also atoms at positions $\mathbf{r}+n_1k_1+n_2k_2+n_3k_3$, where n_1, n_2 and n_3 are arbitrary integers. A remarkable property of PBC is that no point in space is treated any more specially than others.

5. Results and discussion

5.1. Post processing

The final stage of the experimental study is the post-processing. Data array produced by the molecular dynamics code of the MAPS program contains values of required variables in the matrix form. The number of values corresponds to a predetermined time interval. In order to calculate the elasticity, there are following parameters needed: pressure and the linear dimensions of the cells at each time point. Data array analysis is automated and performed by the firmware code, but operator is still required to set up the coordinate system and control the accuracy of the calculation. The program calculates the strain value at each point of time and returns the function of pressure versus strain of the simulated volume. As this dependence in most cases is non-linear, a linear function is found by means of interpolation in the form $y=kx+b$. Since Young's modulus equals

$$E_{ii} = \frac{P_{ii} \cdot L_i}{\Delta l_i}, \tag{17}$$

where $i=x, y, z$; P_{ii} is the pressure along the i-axis; L_i is the original length of the simulation cell along the i-axis and Δl_i is the length variation modulus along the i-axis. Then the coefficient k is numerically equal to the value of Young's modulus in the pressure and strain coordinate system (see an example in Fig. 3).

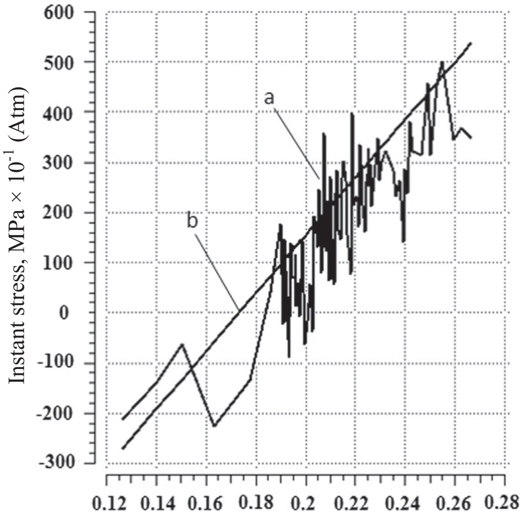

Fig. 3. (a) Stress versus strain simulation result for $C_{24}H_{50}$ (force direction along x-axis, $T=100$ °C); and (b) linearized dependence, $k=0.52$

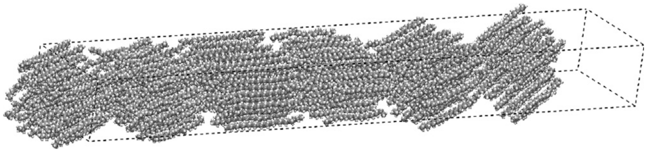

Fig. 4. Relaxed structure of $C_{24}H_{50}$ (simulation time: 60 ps).

Poisson's ratio is calculated using values of the longitudinal and transverse strain as follows

$$\nu_{ij} = -\frac{\Delta l_j \cdot L_i}{L_j \cdot \Delta l_i}, \tag{18}$$

where $i=x$, $j=y$, z; L_i and L_j are the original lengths of the simulation cell along i- and j-axis, respectively; Δl_i and Δl_j are the length variation moduli along i- and j-axis, respectively. An example of the relaxed structure is given in Fig. 4.

The shear modulus G_{ij} is calculated on the same principle as Young's modulus.

According to Kotelnikova and Filatov (2002), hydrocarbon molecules due to thermal exposure can perform a phase transition and form various types of rotational isomers, and their symmetry increases to hexagonal. Then the number of elastic constants reduces down to five, and the matrix of elasticity becomes (Nye, 1985; Ding et al., 2006).

$$C_H = \begin{vmatrix} c_{11} & c_{12} & c_{13} & 0 & 0 & 0 \\ c_{12} & c_{11} & c_{13} & 0 & 0 & 0 \\ c_{13} & c_{13} & c_{33} & 0 & 0 & 0 \\ 0 & 0 & 0 & c_{44} & 0 & 0 \\ 0 & 0 & 0 & 0 & c_{44} & 0 \\ 0 & 0 & 0 & 0 & 0 & c_{66} \end{vmatrix}. \tag{19}$$

According to Eq. (19), the elastic properties of hydrocarbons are identical along both x- and y-axis and unique along z-axis. Thus, the plane $z0x$ becomes the plane of anisotropy.

Elastic constants in Eq. (19) can be found by using the following well known formulas (Ding et al., 2006):

$$c_{11} = \frac{E_{xx}\left(E_{zz} - E_{xx}\nu_{xz}^2\right)}{\left(1+\nu_{xy}\right)\left(E_{zz} - E_{zz}\nu_{xy} - 2E_{xx}\nu_{xz}^2\right)}, \tag{20}$$

Table 3
Young's modulus, shear modulus and Poisson's ratio of some n-paraffins.

Hydrocarbon	Syngony	Temperature (°C)	E_{xx} (E_{yy}) (GPa)	ν_x/ν_y	E_{zz} (GPa)	ν_z	$G_{xz/zx}$ (GPa)
$C_{19}H_{40}$	Orthorhombic	25	0.5	−0.5	2.8	−0.03	0.3
		60	0.2	−0.5	1.4	−0.7	0.15
		100	0.1	−0.5	1	−0.7	0.1
$C_{24}H_{50}$	Triclinic	25	0.6	−0.5	4.1	0.1	0.3
		60	0.3	−0.5	2.1	0.1	0.5
		100	0.5	−0.5	2.4	0.4	0.2
$C_{36}H_{74}$	Orthorhombic	25	–	–	7	0.05	0.25
		60	–	–	3	–	0.7
		100	0.4	−0.5	2.2	−0.02	0.13

$$c_{12} = \frac{E_{xx}\left(E_{zz}\nu_{xy} + E_{xx}\nu_{xz}^2\right)}{\left(1+\nu_{xy}\right)\left(E_{zz} - E_{zz}\nu_{xy} - 2E_{xx}\nu_{xz}^2\right)}, \tag{21}$$

$$c_{13} = \frac{E_{xx}E_{zz}\nu_{xz}}{E_{zz} - E_{zz}\nu_{xy} - 2E_{xx}\nu_{xz}^2}, \quad c_{33} = \frac{E_{zz}^2\left(1-\nu_{xy}\right)}{E_{zz} - E_{zz}\nu_{xy} - 2E_{xx}\nu_{xz}^2}, \tag{22, 23}$$

$$c_{44} = G_{xz}, \quad c_{66} = \frac{c_{11} - c_{12}}{2}. \tag{24, 25}$$

5.2. Numerical results and their physical implication

Some interesting results were obtained for crystals with the orthorhombic type of symmetry. Table 3 contains calculated values of the elasticity parameters of n-paraffins at three different temperatures. Among these values a particular interest is drawn by Poisson's ratio which possesses the negative value almost in all cases.

Organic auxetics are known in modern science. Thus, the authors He et al. (1998) and Kang et al. (1999) have shown that in nematic liquid crystals with parallel orientation of molecular axes the negative Poisson's ration effect is possible. Taking into account the latest concept of petroleum as a liquid-crystalline substance (see for example, Han et al., 2008; Bagheri et al., 2010), a negative Poisson's ratio is expectable. However, there are no direct experimental proofs for a negative Poisson's ratio of n-paraffins available.

Dependence of Young's modulus on the number of carbon atoms in paraffin crystal monomers is shown in Fig. 5. In order to provide a reference point, the value for n-paraffin C_8H_{18} was obtained from simulation as well. However, this n-paraffin was not included into a complex research, as its melting point corresponds to −216.15 K; and generalized Hook's law becomes meaningless at the temperatures used in simulation experiments.

It can be noted that the diagram has a linear form. Obviously, the stiffness of saturated hydrocarbons is directly proportional to the number of carbon molecules in their chains.

The elastic behavior of n-paraffins in a wide temperature range is shown in Fig. 6. It can be noted that for all the three models the change in elasticity has a non-linear form. This is the evidence of the phase transition process which physically takes place in saturated (and unsaturated) hydrocarbons medium. According to diagrams in Fig. 6, the phase transition process ends at the temperature of 60–65 °C. Phase transition is also expected for the temperatures, the values of which are outside the current experimental range.

5.3. Model verification/validation

For the purpose of verification of the values of Young's and shear moduli listed in Table 3, we shall define the elasticity parameters of some particular petroleum products, and then compare them with the available data.

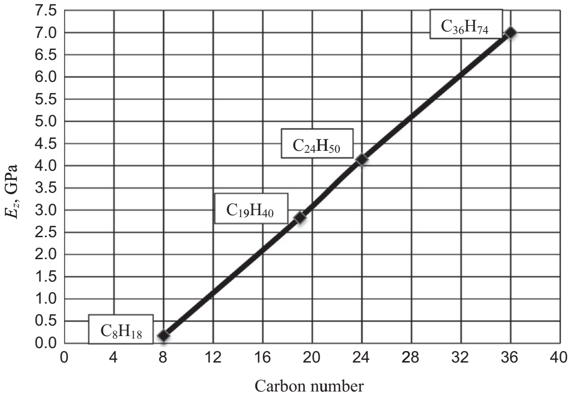

Fig. 5. Young's modulus in anisotropy plane of some n-paraffin crystals (T=25 °C).

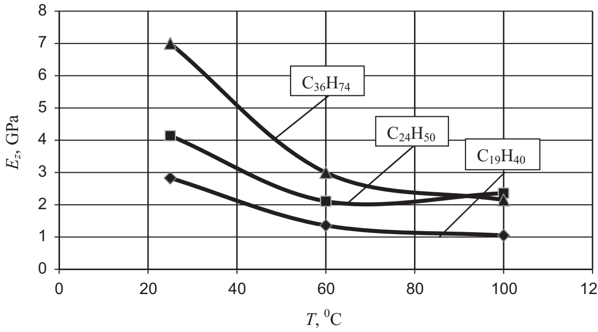

Fig. 6. Young's modulus of some n-paraffins in anisotropy plane versus temperature.

Speight (2014) defines diesel oil as a No. 2 fuel (refinery specification), whose composition consists of aliphatic hydrocarbons (64%), unsaturated hydrocarbons (1–2%) and aromatic hydrocarbons (35%). Their chain length remains in the C_{11}–C_{20} range. Then an average carbon atom with respect to concentration can be found as C_{14} (C_{13}) due to the lower boiling temperature of smaller chains (Leffler, 1985). Using the diagram in Fig. 5, the bulk modulus of liquid diesel oil can be estimated: E=1.6 GPa (1.4 GPa). Handbooks in hydraulics list the following values for the bulk modulus of diesel oil: 1.4–1.45 GPa. Thus, the discrepancy range of the simulated values of Young's modulus becomes 0–12.5%. Aromatic hydrocarbons were treated as small alkanes in this case.

Also Speight (2014) reported that residual fuel oil is called No. 6 fuel oil, and its composition is not well known yet. It is obtained

Table 4
Comparison of experimental vs. calculated values of elastic parameters of two petroleum products.

Heavy oil		Diesel oil	
Parameter	Value	Parameter	Value
Young's modulus (MD modeling) (GPa)	3	Bulk modulus (MD modeling) (GPa)	1.6
Young's modulus (experiment) (GPa)	2.85	Bulk modulus (experiment) (GPa)	1.4
Relative deviation (%)	5	Relative deviation (%)	12.5
Shear modulus (MD modeling) (GPa)	0.3	–	–
Shear modulus (experiment) (GPa)	0.25	–	–
Relative deviation (%)	16.7	–	–

after the removal of the light fractions of a crude oil. No. 6 fuel oil can be blended directly to heavy fuel oil or made into asphalt. Residual fuel oil is more complex in composition and impurities than distillate fuels.

Taking into consideration that hydrocarbons chain length now should remain in the C_{20}–C_{50} range (Hodges, 1996; Speight, 2014), the composition of heavy oil can be estimated using three hydrocarbons from this study. As in the first case, the concentration is higher for the n-paraffins with smaller carbon number. The composition expression can be written as

$$\text{HFO} = 40\% C_{19}H_{40} + 45\% C_{24}H_{50} + 15\% C_{36}H_{74}, \tag{26}$$

where summands are multiplied by their predictive concentration values.

According to Eq. (26) and Table 3, the values of Young's and shear moduli at the temperature of 25 °C become 3 GPa and 0.3 GPa, respectively. These values can be compared with the results from the work by Han et al. (2008). The authors have obtained the values of the bulk and shear moduli for an API 8 (1010.8 kg/m^3) gravity heavy oil using ultrasonic wave propagation time measuring method. The values reported at the temperature of 25 °C were 2.85 GPa for the bulk modulus and 0.25 GPa for the shear modulus. Nevertheless, some clarification is needed here. The authors reported the values of the bulk modulus, but in fact they were measuring Young's modulus. This comes from the experiment description part of their paper where the P-wave time propagation measuring method is described. Since the authors treat heavy oil as a substance with non-liner shear elasticity, the bulk modulus, in this case, becomes a function of Young's and shear moduli.

The summary of the molecular dynamics model validation is given in Table 4. It can be seen that the relative deviation is much less for Young's modulus of heavy oil than for its shear modulus. Nevertheless, even though the composition of heavy oil was estimated roughly, such an agreement with experiment indicates a qualitative molecular dynamics study.

Besides fuel oils, lubricating and hydraulic oils there are other petroleum products. According to Hodges (1996), a major type of hydraulic fluid is the mineral oil class of hydraulic fluids. Mineral-based oils are produced from heavy-end crude oil distillates. Hydrocarbon numbers ranging from C_{15} to C_{50} occur in the various types of mineral oils, with the heavier distillates having higher percentages of the higher carbon number compounds. Hružík et al. (2013) reported the experimentally measured bulk modulus of elasticity of hydraulic oil. However, the grade of oil was not mentioned. The value obtained was 1.73 GPa, at the temperature of 20 °C. This value corresponds to C_{14}–C_{15} in Fig. 5. Obviously, the authors were using low viscosity hydraulic oil in their experiments.

5.4. *Determination of elasticity matrix for the heavy oil product*

Finally, let us estimate the elasticity matrix of a heavy petroleum product at the temperature of 100 °C. Such temperature level is essential for the engineering industry, since heavy petroleum products are normally heated up before they can be pumped and/or injected into combustion chambers. Using Eqs. (19)–(26) and Table 3, the elasticity matrix of heavy fuel oil can be defined as

$$C_F = \begin{vmatrix} 0.43 & -0.21 & 0.05 & 0 & 0 & 0 \\ -0.21 & 0.43 & 0.05 & 0 & 0 & 0 \\ 0.05 & 0.05 & 3.82 & 0 & 0 & 0 \\ 0 & 0 & 0 & 0.13 & 0 & 0 \\ 0 & 0 & 0 & 0 & 0.13 & 0 \\ 0 & 0 & 0 & 0 & 0 & 0.32 \end{vmatrix}. \tag{27}$$

The elasticity matrix (27) is applicable for a heavy oil fuel product enclosed in a cylindrical body which has a longitudinal dimension bigger than a diametric one. For example, a pipeline. Then the anisotropy axis of paraffins will be aligned with the pipe axis, as demonstrated (Venkatesan et al., 2005). As it can be seen from Eq. (27), the elasticity of heavy oil in the anisotropy plane is much higher (10 times) than in the planes of isotropy. Shear elasticity is rather small and remains around 0.1 GPa at this temperature. The negative values of tangential components in Eq. (27) are explained by the liquid-crystalline nature of heavy petroleum products. The stability of the materials with negative elastic constants is proven to be possible in a condition of both full and partial constraint (Wang and Lakes, 2005).

6. Conclusions

Both expected and unexpected results have been obtained during molecular dynamics simulation study of saturated hydrocarbons. It appears that their elasticity is a complex term. It can be described as the function of the chemical structure of n-paraffins and their energy state, i.e. the temperature level.

The numerical results obtained for the elastic parameters of some normal paraffins using molecular dynamics simulation method suggest that their elastic properties are closer in nature to the properties of nematic liquid crystals rather than amorphous entities. Special attention was drawn by the negative Poisson's ratio values. Paraffins, after the proper experimental verification of this effect, could be ranked as auxetic materials. This would open a new page in understanding hydrocarbons elasticity.

The experimental verification of Young's and shear moduli has shown a good agreement between simulated and measured numerical results earlier reported by Han et al. (2008) and Hružík et al. (2013).

The matrix of elasticity of a highly viscous (heavy) oil product was estimated at the temperature of 100 °C. The matrix can reflect the elastic behavior of oil products in a certain temperature range defined by the presented results. The matrix of a heavy petroleum product elasticity has an important direct application. It may be used to obtain more qualitative results when performing seismic oil exploration research; also it may be used by individual researchers or research groups to improve hydro-dynamical, wave field and critical strain engineering calculations for the heavy oil products pumping systems, since oil products are often considered as plain fluids in the governing equations of such calculations.

It can be concluded that the technique of assessing the elasticity of complex chemical substances proposed in this paper is sufficiently reliable and accurate. The technique consists in estimating the elasticity of a complex substance by identifying and determining the elastic properties of its individual components, followed by an averaged result according to the chemical composition of a particular substance.

References

Bagheri, S.R., Bazyleva, A., Gray, M.R., McCaffrey, W.C., Shaw, J.M., 2010. Observation of liquid crystals in heavy petroleum. Energy Fuels 24 (8), 4327–4332. http://dx.doi.org/10.1021/ef100376t.

Cornell, W.D., Cieplak, P., Bayly, C., Gould, I., Merz, K., Ferguson, D., Spellmeyer, D., Fox, T., Caldwell, J., Kollman, P., 1995. A second generation force field for simulations of proteins, nucleic acids, and organic molecules. J. Am. Chem. Soc. 117 (19), 5179–5197. http://dx.doi.org/10.1021/ja00124a002.

Diallo, M.S., Cagin, T., Faulon, J.L., Goddard III, W.A., 2000. Thermodynamic properties of asphaltenes: a predictive approach based on computer assisted structure elucidation and atomistic simulations. Asphaltenes and asphalts, 2. Dev. Pet. Sci. 40 (Part B), 103–127. http://dx.doi.org/10.1016/s0376-7361(09)70276-6 (Chapter 5).

Ding, H., Chen, W., Zhang, L., 2006. Elasticity of Transversely Isotropic Materials. Solid Mechanics and Its Applications, vol. 126, Dordreht. Springer p. 443. http://dx.doi.org/10.1007/1-4020-4034-2.

Field, M., 2007. A Practical Introduction to the Simulation of Molecular Systems, 2nd ed. Cambridge University Press, New York p. 344. http://dx.doi.org/10.1017/cbo9780511619076.

Han, D.-H., Liu, J., Batzle, M., 2008. Seismic properties of heavy oils-measured data. Lead. Edge 27 (9), 1108–1115. http://dx.doi.org/10.1190/1.2978972.

He, C., Liu, P., Griffin, A., 1998. Toward negative Poisson ratio polymers through molecular design. Macromolecules 31 (9), 3145–3147. http://dx.doi.org/10.1021/ma970787m.

Hodges, P.K.B, 1996. Hydraulic Fluids. Elsevier, Oxford, Burlington p. 188.

Hružík, L., Vašina, M., Bureček, A., 2013. Evaluation of bulk modulus of oil system with hydraulic line. In: Proceedings of EPJ Web of Conferences, vol. 45, 01041. http://dx.doi.org/10.1051/epjconf201/20134501041.

Jorgensen, W.L., Maxwell, D.S., Tirado-Rives, J., 1996. Development and testing of the OPLS all-atom force field on conformational energetics and properties of organic liquids. J. Am. Chem. Soc. 118 (45), 11225–11236. http://dx.doi.org/10.1021/ja9621760.

Kang, D., Mahajan, M.P., Zhang, S., Petschek, R.G., Rosenblatt, C., He, C., Griffin, A.C., 1999. Pretransitional behavior above the nematic–isotropic phase transition of an auxetic trimmer liquid crystal. Phys. Rev. E 60 (4), 4980–4982. http://dx.doi.org/10.1103/PhysRevE.60.4980.

Kotelnikova, Ye.N., Filatov, S.K., 2002. Crystal Chemistry of Paraffins: Methods, Researches, Results, Behavior in Nature. Zhurnal Neva, St. Petersburg (in Russian).

Leffler, W.L., 1985. Petroleum Refining for the Nontechnical Person, 2nd ed. PennWell Books, Tulsa.

MacKerell, A.D., et al., 1998. All-atom empirical potential for molecular modeling and dynamics studies of proteins. J. Phys. Chem. B 102 (18), 3586–3616. http://dx.doi.org/10.1021/jp973084f.

Martyna, G., Tobias, D., Klein, M., 1994. Constant pressure molecular dynamics algorithms. J. Chem. Phys. 101 (5), 4177–4189. http://dx.doi.org/10.1063/1.467468.

Mayo, S., Olafson, B., Goddard III, W.A, 1990. DREIDING: a generic force field for molecular simulations. J. Phys. Chem. 94 (26), 8897–8909. http://dx.doi.org/10.1021/j100389a010.

Nye, J.F., 1985. Physical Properties of Crystals: Their Representation by Tensors and Matrices. Oxford University Press, Oxford.

Plimpton, S., 1995. Fast parallel algorithms for short-range molecular dynamics. J. Comp. Phys. 117 (1), 1–19. http://dx.doi.org/10.1006/jcph.1995.1039.

Rapp´e, A.K., Casewit, C.J., Colwell, K.S., Goddard III, W.A., Skiff, W.M., 1992. UFF, a full periodic table force field for molecular mechanics and molecular dynamics simulations. J. Am. Chem. Soc. 114 (25), 10024–10035. http://dx.doi.org/10.1021/ja00051a040.

Shinoda, W., Shiga, M., Mikami, M., 2004. Rapid estimation of elastic constants by molecular dynamics simulation under constant stress. Phys. Rev. B 69 (13), 134103. http://dx.doi.org/10.1103/PhysRevB.69.134103.

Speight, J., 2014. The Chemistry and Technology of Petroleum, 5th ed. CRC Press, Boca Raton, London, New York p. 913. http://dx.doi.org/10.1201/9780824742119.

Sun, H., 1998. COMPASS: an ab initio force-field optimized for condensed-phase applications—overview with details on alkane and benzene compounds. J. Phys. Chem. B 102 (38), 7338–7364. http://dx.doi.org/10.1021/jp980939v.

Venkatesan, R., Nagarajan, N.R., Paso, K., Yi, Y.-B., Sastry, A.M., Fogler, H.S., 2005. The strength of paraffin gels formed under static flow. Chem. Eng. Sci. 60 (13), 3587–3598. http://dx.doi.org/10.1016/j.ces.2005.02.045.

Wang, Y.C., Lakes, R.S., 2005. Composites with inclusions of negative bulk modulus: extreme damping and negative Poisson's ratio. J. Compos. Mater. 39 (18), 1645–1657. http://dx.doi.org/10.1177/0021998305051112.

Yip, S., 2005. Handbook of Materials Modeling. Part B. Models. Springer, Dordrecht, Berlin, Heidelberg, New Yorkhttp://dx.doi.org/10.1007/1-4020-3286-2.